Combined N- and C-Terminal Truncation of Human Apolipoprotein A-I Yields a Folded, Functional Central Domain†

Jennifer A. Beckstead,‡ Brian L. Block,‡ John K. Bielicki,§ Cyril M. Kay,|| Michael N. Oda,‡ and Robert O. Ryan*,‡

Lipid Biology in Health and Disease Research Group, Children's Hospital Oakland Research Institute, 5700 Martin Luther King Jr. Way, Oakland, California 94609, Department of Biochemistry and Protein Engineering, Network of Centres of Excellence, University of Alberta, Edmonton, Alberta, Canada T6G 2H7, and Genome Sciences Department, Life Science Division, Lawrence Berkeley National Laboratory, Berkeley, California 94720

Received October 26, 2004; Revised Manuscript Received January 10, 2005

ABSTRACT: A combined N- and C-terminal truncation variant of human apolipoprotein A-I (apoA-I) was designed, expressed in *Escherichia coli*, isolated, and characterized. Hydrodynamic experiments yielded a weight average molecular weight of 34000, indicating apoA-I-(44−186) exists in solution predominantly as a dimer. An axial ratio of 4.2 was calculated for the dimer based on sedimentation velocity experiments. Far-UV circular dichroism spectroscopy of apoA-I-(44−186) in buffer indicated the presence of 65% α-helix secondary structure. Guanidine hydrochloride denaturation experiments yielded a transition midpoint of 0.5 M for apoA-I-(44−186). ApoA-I-(44−186) induced solubilization of dimyristoylphosphatidylcholine vesicles at a rate comparable to that of full-length apoA-I, displayed lipoprotein binding ability, and was an acceptor of ABCA1-mediated cholesterol efflux from cultured macrophages. Fluorescence quenching studies with KI indicate that the three Trp residues in apoA-I-(44−186) are shielded from the aqueous environment. Taken together, the data indicate that lipid-free apoA-I-(44−186) adopts a folded conformation in solution that possesses lipid binding capability. The central region of apoA-I appears to adopt a globular amphipathic α-helix bundle organization that is stabilized by intramolecular and/or intermolecular helix−helix interactions. Lipid association likely results in a conformational adaptation wherein helix−helix contacts are substituted for helix−lipid interactions.

Human apolipoprotein A-I (apoA-I) is a 243 amino acid protein that is a major component of high-density lipoprotein (HDL).[1] Lipid-poor apoA-I is a physiologically relevant acceptor of cell-derived cholesterol via the ATP binding cassette transporter A1 (ABCA1). Nascent lipoproteins comprised of apoA-I, cholesterol, and phospholipid are substrates for lecithin:cholesterol acyl transferase (LCAT) mediated production of cholesteryl ester, a key step in the generation of core-containing HDL particles. In its capacity as a structural component of HDL, a modulator of LCAT activity and ligand for ABCA1-dependent cholesterol efflux, apoA-I is a central figure in the reverse cholesterol transport pathway. Numerous studies have been conducted to characterize structure and function relations in apoA-I. In a manner similar to that of other apolipoproteins, it has been proposed that lipid-free human apoA-I possesses a helix bundle structural motif (*1*, *2*).

Strategies employed to investigate the structural organization of apoA-I have included N-terminal truncation, C-terminal truncation, helix substitution, and helix swapping. Truncation of apoA-I at the C-terminus to yield apoA-I-(1−192) results in a protein with decreased lipid binding ability (*3*). Unlike full-length apoA-I, C-terminal truncated apoA-I exists as monomers and dimers in solution. The N-terminal 43 amino acids of apoA-I are encoded by a distinct exon, and secondary structure predictions indicate that this region of the molecule is unique in that it is composed of a class G* amphipathic α-helix (*4*). N-Terminal truncation of apoA-I to generate apoA-I-(44−243) yields a protein with altered solution structure characteristics. Evidence was obtained that removal of residues 1−43 of apoA-I induces a conformation that is proposed to be reminiscent of the conformation adopted upon lipid interaction of intact apoA-I (*5*, *6*). Consistent with this, Borhani et al. (*7*) reported the X-ray crystal structure of lipid-free apoA-I-(44−243) and showed that it exists as a horseshoe-shaped series of amphipathic α-helices that sequester their hydrophobic faces through helix−helix contacts in a tetrameric arrangement of truncated apoA-I molecules. Recent studies of lipid-associated apoA-I have provided support for the concept that, in phospholipid disk complexes, apoA-I exists as an extended series of α-helices that circumscribe the perimeter of a disk-shaped phospholipid bilayer such that the α-helix segments align perpendicular to the fatty acyl chains of the bilayer phospholipids (*8*−*10*). In this orientation the hydrophobic face of individual α-helices interacts with lipid molecules at the edge of the disk.

† Supported by grants from the NIH (HL-64159) and the American Heart Association (0235222N).

* Address correspondence to this author. Tel: 510-450-7645. Fax: 510-450-7910. E-mail: rryan@chori.org.

‡ Children's Hospital Oakland Research Institute.

§ Lawrence Berkeley National Laboratory.

|| University of Alberta.

[1] Abbreviations: apo, apolipoprotein; HDL, high-density lipoprotein; ABCA1, ATP binding cassette transporter A1; LCAT, lecithin: cholesterol acyl transferase; ANS, 8-anilino-1-naphthalenesulfonic acid; CD, circular dichroism; DMPC, dimyristoylphosphatidylcholine.

10.1021/bi0477135 CCC: $30.25
Published on Web 02/19/2005

In studies of lipid-free apoA-I, Jonas and co-workers used fluorescence spectroscopy to obtain evidence that the N- and C-termini of apoA-I are in close proximity to one another (*11*). On the basis of the results of Oda et al. (*12*) wherein it was shown that the C-terminus of apoA-I functions as a lipid-triggered molecular switch, it is conceivable that the "trigger" mechanism is held in check in the absence of lipid through interactions with the N-terminus. If so, it is reasonable to consider that the remaining central region of apoA-I is organized as a helix bundle that is poised to undergo a lipid binding induced conformational transition similar to that reported for the apoE N-terminal domain (*13*) and apolipophorin III (*14*). In the present study, we hypothesized that truncation of both the N- and C-termini would yield a stable fragment that constitutes a core structural element of apoA-I. The results obtained indicate that, in the absence of the C-terminal residues 187−243, removal of residues 1−43 does not induce a major structural reorganization while retaining a protein fold that is consistent with a globular amphipathic α-helix bundle.

EXPERIMENTAL PROCEDURES

Plasmid Construction. The Bluescript KS(+) plasmid vector harboring the coding sequence of human apoA-I (*16*) was employed as a template for gene amplification. Oligonucleotide primers containing nonannealing *Cla*I and *Xba*I sites were designed to amplify the nucleotide sequence encoding residues 44−186 of apoA-I. The amplification product was digested with *Cla*I and *Xba*I and subcloned into a Bluescript KS(+) vector digested with the same enzymes and transformed into DH5α cells. The apoA-I-(44−186)/Bluescript vector construct included a 17-residue N-terminal His-tag extension together with an engineered thrombin cleavage site adjacent to the beginning of the apoA-I sequence (*15*). For protein expression the apoA-I-(44−186) cDNA was subcloned into the pET20b+ plasmid and transformed into BL21(DE3) pLysS cells.

Bacterial Expression and Purification of ApoA-I-(44−186). ApoA-I-(44−186) expression and purification were performed as described by Ryan et al. (*15*). Dialysis into 20 mM Tris-HCl, pH 8.0, and digestion with a 1:100 ratio of thrombin:apoA-I-(44−186) for 3 h at 37 °C induce cleavage of the 17-residue N-terminal His-tag extension. The digested protein contains a six-residue N-terminal extension (GSIDDP-). Aside from this adduct, the protein corresponds directly to residues 44−186 of human apoA-I, comprising a total of 149 amino acids. The digestion products were further purified on a Perkin-Elmer Series 200 high-pressure liquid chromatograph. The sample was applied to a semipreparative RXC-8 Zorbax 300SB column and eluted with a linear AB gradient of 2% solvent B per minute, where solvent A was 0.05% trifluoroacetic acid in water and solvent B was 0.05% trifluoroacetic acid in acetonitrile. Fractions were monitored at 230 nm, and those corresponding to apoA-I-(44−186) were pooled, lyophilized, and stored at −20 °C. Full-length human apoA-I was expressed and purified as described earlier (*15*).

Analytical Procedures. Protein concentrations were determined using the bicinchoninic acid assay (Pierce Chemical Co.) using bovine serum albumin as standard. SDS−PAGE was performed on 4−20% acrylamide slab gels run at a constant 30 mA for 1.5 h. Gels were stained with Gel Code (Pierce Chemical Co.) stain according to the manufacturer's instructions. Mass spectrometry was performed on a Bruker Autoflex MALDI-TOF instrument equipped with a SCOUT MTP ion source. Samples were spotted onto a Scout 384 plate using a matrix of sinapinic acid saturated in 30% acetonitrile/70% water/0.1% trifluoroacetic acid. Ions were accelerated at +20 kV, and masses were detected in linear mode with protein A used as an external calibrant.

Fluorescence Spectroscopy. Fluorescence spectra were obtained on a Perkin-Elmer LS 50B luminescence spectrometer. For quenching studies samples were excited at 295 nm, and emission was monitored from 300 to 350 nm. A stock solution of potassium iodide contained 1 mM thiosulfate to prevent formation of free iodine. Quenching data were analyzed by the Stern−Volmer equation: $F_0/F = 1 + K_{sv}$-[Q], where F_0 and F represent the emission maximum in the absence and presence of quencher, respectively. The collisional quenching constant, K_{sv}, was determined from the slope of plots of F_0/F versus [Q]. In other studies, spectra of 8-anilino-1-naphthalenesulfonic acid (ANS) solutions were obtained in 10 mM sodium phosphate buffer (pH 7.0) and in the presence of 3 μM full-length apoA-I or apoA-I-(44−186). Since ANS fluorescence in buffer is negligible (*17*), spectra were recorded in a excess of ANS with respect to protein (mole per mole). Samples were excited at 395 nm with emission monitored from 400 to 600 nm (3 nm slit width).

Analytical Ultracentrifugation. Sedimentation equilibrium experiments were conducted at 20 °C in a Beckman XL-I analytical ultracentrifuge using absorbance optics, as described by Laue and Stafford (*18*). Aliquots (110 μL) of the sample solution were loaded into six-sector CFE sample cells, allowing three concentrations to be run simultaneously. Runs were performed at a minimum of two different speeds, and each speed was maintained until there was no significant difference in $r^2/2$ versus absorbance scans taken 2 h apart to ensure that equilibrium was achieved. Sedimentation equilibrium data were evaluated using the NONLIN program, which employs a nonlinear least squares curve-fitting algorithm described by Johnson et al. (*19*). The program allows for analysis of both single and multiple data files and can be fit to models containing up to four associating species, depending upon which parameters are permitted to vary during the fitting routine. The protein's partial specific volume and the solvent density were estimated using the Sednterp program (*20*). Sedimentation velocity experiments were run at 40000 rpm and 20 °C using absorbance optics. Up to 260 scans were performed during the run. A sedimentation coefficient value was obtained by analyzing 10 sets of data selected between the 160th and 205th scan using the Svedberg software. From the amino acid composition, a hydration value of 0.44 was obtained, assuming that all charged groups are exposed.

Far-UV Circular Dichroism Spectroscopy. Far-UV circular dichroism (CD) measurements were performed on a Jasco J-720 spectropolarimeter using Jasco J-700 Hardware Manager software. The spectropolarimeter was routinely calibrated using a 0.06% (w/v) aqueous solution of ammonium *d*-camphorsulfonate at 290.5 nm. Scans were performed using a 0.02 cm path length and a protein concentration of 4.3 μM. The sample chamber was maintained at 25 °C using

a Lauda RM6 refrigerated water bath. Samples were dissolved in 50 mM sodium phosphate, pH 7.0, and 100 mM NaCl. The concentrations of apoA-I-(44−186) stock solutions were determined hydrodynamically as described by Babul and Stellwagen (*21*). For guanidine hydrochloride denaturation experiments, samples were incubated overnight at a given denaturant concentration in order to attain equilibrium. Baseline correction, noise reduction, and ellipticity calculations were carried out using Jasco J-700 for Windows Standard Analysis software. The values are shown as mean residue ellipticity (millidegrees squared per centimenter per decimole) using a mean residue weight value of 116.7. Deconvolution was performed on the scans using the Contin program of Provencher and Glöckner (*22*).

Lipid Binding Studies. Bilayer vesicles of dimyristoylphosphatidylcholine (DMPC) were prepared by extrusion through 200 nm filters as described by Weers et al. (*23*). Protein and lipid vesicles were prepared in 20 mM sodium phosphate, pH 7.0. Six hundred nanomoles of DMPC vesicles were incubated at 24 ° C in a thermostated cell holder in the absence or presence of 6 nmol of apolipoprotein (sample volume = 400 μL). Sample right angle light scattering intensity was monitored on a Perkin-Elmer LS 50B luminescence spectrometer, with the excitation and emission monochromators set at 600 nm (2.8 nm slit width).

Lipoprotein Binding Assay. Human low-density lipoprotein (LDL) was incubated for 60 min at 37 °C in the presence of *Bacillus cereus* phospholipase C (PL-C) (0.33 unit/50 μg of LDL protein). Where indicated, apolipoprotein, from 0 to 50 μg/50 μg of LDL protein, was included in the reaction mixture. Incubations were conducted in 50 mM Tris-HCl, pH 7.5, 150 mM NaCl, and 2 mM $CaCl_2$ in a total sample volume of 300 μL. Sample absorbance at 340 nm was determined on a Spectramax 340 microtiter plate reader.

Cellular Cholesterol Efflux. J774 macrophages were used to assess the cholesterol efflux properties of apoA-I-(44−186). This cell line was chosen because cholesterol efflux can be enhanced using a cAMP analogue which upregulates ABCA1 protein expression. The cells were seeded onto 24-well culture plates and labeled for 48 h with [^{3}H]cholesterol in RPMI-1640 supplemented with 1% fetal bovine serum. The cAMP analogue, 8-(4-chlorophenylthio)adenosine 3′,5′-cyclic monophosphate, was added (0.3 mM, final concentration) to the cells at least 12 h prior to the initiation of cellular cholesterol efflux. ApoA-I-(44−186) was used in lipid-free form added to serum-free RPMI medium to yield a final concentration of 50 μg/mL. The lipid-free form of full-length recombinant apoA-I was used (50 μg/mL) as a positive control to define apparent ABCA1-dependent cholesterol efflux in the presence and absence of cAMP stimulation. Efflux results were expressed as a percentage of the initial cellular [^{3}H] appearing in the medium as a function of time subtracting the background efflux obtained using serum-free medium alone.

RESULTS

Bacterial Expression and Characterization of ApoA-I-(44−186). A plasmid vector generated for optimized bacterial expression of full-length human apoA-I was reengineered to permit expression of a truncated apoA-I variant. Compared to full-length human apoA-I, the truncated molecule is missing residues 1−43 and 187−243. As with full-length apoA-I production using this expression system, the yield of apoA-I-(44−186) was approximately 50 mg/L of bacterial culture. Figure 1 shows SDS−PAGE analysis of sample purity and the effect of thrombin digestion on the relative mobility of apoA-I-(44−186). MALDI-TOF mass spectrometry analysis of HPLC-purified apoA-I-(44−186) yielded a molecular weight of 17457 ± 13 (n = 7), in agreement with the expected 17388. The isolated protein was stored salt-free as a lyophilized powder at −20 °C. Whereas full-length human apoA-I stored in this manner must be redissolved in urea or guanidine hydrochloride initially (*1*), followed by dialysis or chromatography to remove the chaotrope, apoA-I-(44−186) did not display this behavior and readily dissolved in buffer at pH 7.0.

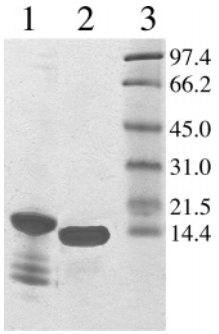

FIGURE 1: SDS−PAGE analysis of apoA-I-(44−186). Lanes: (1) post Ni^{2+} chelation column eluate; (2) thrombin digested apoA-I-(44−186) eluted from semipreparative reversed-phase HPLC; (3) molecular mass standards (kDa).

Self-Association Properties. C-Terminal truncation of apoA-I results in a product that exists as monomers and dimers in the absence of lipid (*3*) while N-terminal truncation alone results in multiple conformers, including an elongated monomeric helical hairpin (*6*). To determine the self-association properties of N- and C-terminal truncated apoA-I in the absence of lipid, hydrodynamic experiments were conducted. Sedimentation equilibrium analyses were performed at 20 °C using absorbance optics. Since the molecular mass of apoA-I-(44−186) is approximately 17 kDa, the initial centrifugation speed was set at 19000 rpm, and equilibrium was reached after 18 h. Data were collected at 19000, 21000, and 23000 rpm (Figure 2). The apparent average molecular mass of apoA-I-(44−186) was 34955 Da, and the data were best fit to a monomer−dimer−tetramer model with most of the sample present in a dimeric state. To evaluate the shape of the truncated apoA-I species, sedimentation velocity experiments were conducted. Using the Svedberg software, the data were fit to a single species model yielding a sedimentation coefficient of 2.62. Sednterp was then used to calculate an axial ratio value. Using a prolate model and a hydration expansion of 17.1%, an axial ratio (a/b) = 4.2 was obtained.

Far-UV CD Studies. The effect of N- and C-terminal truncation on the secondary structure content of apoA-I was evaluated by far-UV CD spectroscopy. In buffer alone, apoA-I-(44−186) gave rise to a spectrum characteristic of high α-helix content (Figure 3). Deconvolution of the spectrum indicated the presence of 65% α-helix, 12% β-sheet, and 23% random plus other conformers. Spectra obtained in the presence of 50% (v/v) trifluoroethanol resulted in additional α-helix, up to 70%. Thus, removal of both the N- and

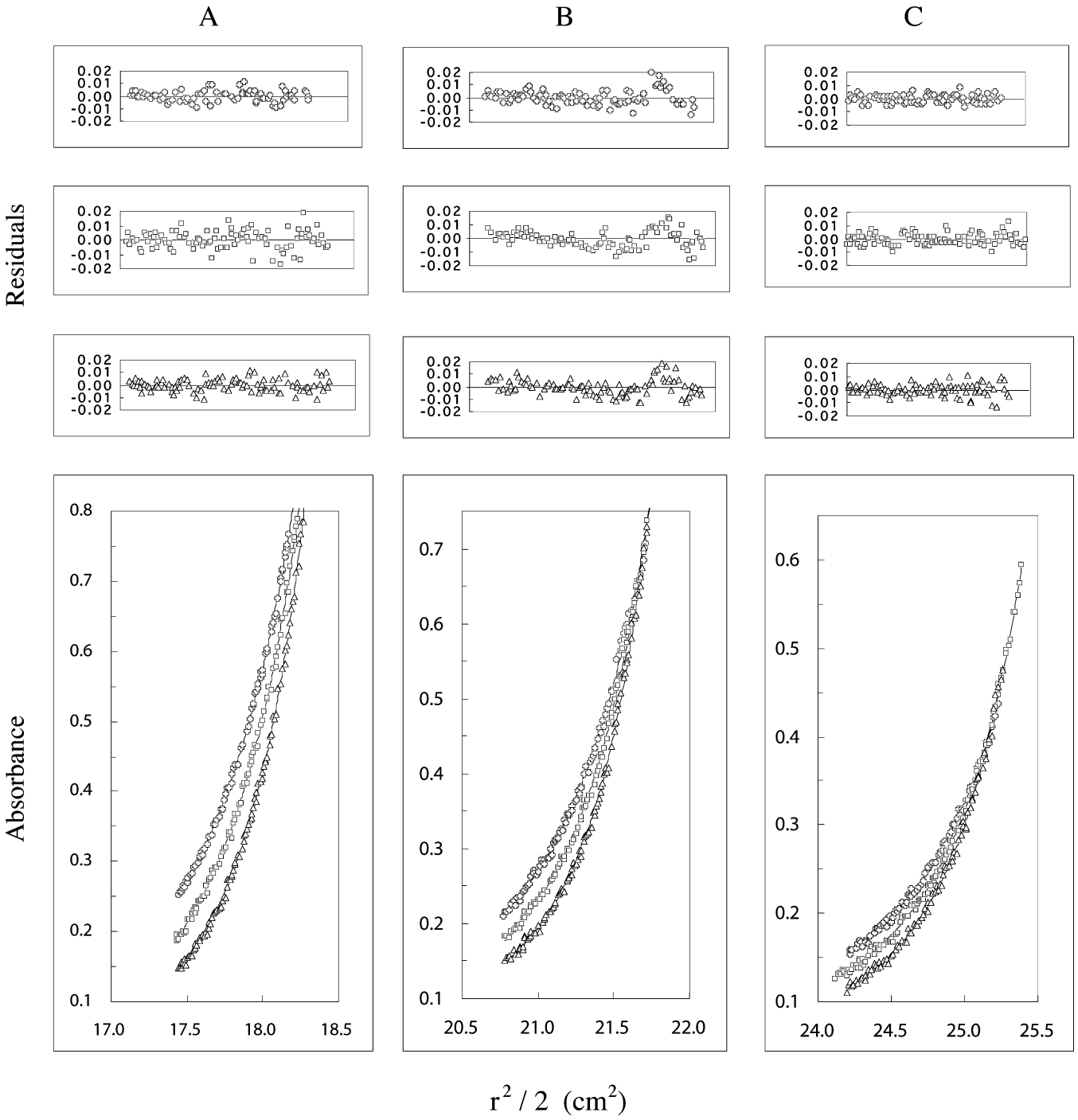

FIGURE 2: Sedimentation equilibrium analysis of apoA-I-(44−186). Protein was dissolved in 20 mM sodium phosphate, pH 7.0, and 100 mM sodium chloride and centrifuged at 19000 rpm (crosses), 21000 rpm (squares), and 23000 rpm (triangles) at 20 °C. The protein concentrations used were 0.55, 0.33, and 0.17 mg/mL for sectors A, B, and C, respectively. Lower panels: $r^2/2$ versus absorbance plots. Symbols represent measured data points, and solid lines represent the fit to a monomer−dimer−tetramer model. Upper panels: Residuals obtained from fitting the measured data points to a three-species model. The random, nonsystematic distribution of the residuals indicates a good fit of the data to the model.

C-terminal segments of apoA-I does not compromise the ability of apoA-I-(44−186) to adopt secondary structure or to respond to the helix-inducing cosolvent, trifluoroethanol, by adopting additional helix content. The stability properties of apoA-I-(44−186) were evaluated in guanidine hydrochloride denaturation experiments monitored by CD spectroscopy. As depicted in the inset to Figure 3, a transition midpoint of 0.5 M was observed.

Fluorescence Properties of ApoA-I−(44−186). The wavelength of maximum fluorescence emission of apoA-I-(44−186) was 346 nm (excitation 280 nm) as compared to 343 nm for wild-type apoA-I. Fluorescence quenching experiments were performed to obtain information about the local environment of Trp residues in apoA-I-(44−186). The effect of increasing amounts of the negatively charged quencher, KI, on the fluorescence emission intensity of wild-type and truncated apoA-I was evaluated. Stern−Volmer plots (Figure 4) yielded a $K_{sv} = 1.5$ for wild-type apoA-I and a value of 1.7 for apoA-I-(44−186). Whereas wild-type apoA-I possesses four Trp residues (at positions 8, 50, 72, and 108),

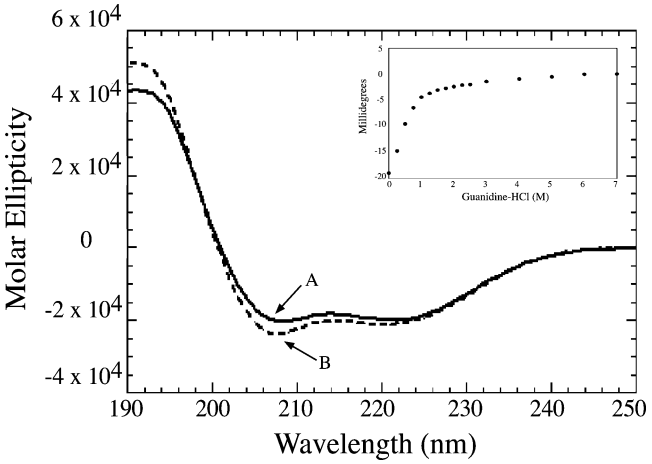

FIGURE 3: Far-UV circular dichroism spectra of apoA-I-(44−186). Spectra were collected at 20 °C in 50 mM sodium phosphate, pH 7.0, and 100 mM NaCl. The protein concentration was 4.3 μM. Curves: (A) apoA-I-(44−186) in buffer; (B) apoA-I-(44−186) in buffer containing 50% trifluoroethanol (v/v). Inset: Effect of guanidine hydrochloride on the secondary structure content of apoA-I-(44−186). Far-UV circular dichroism, monitored as millidegrees at 222 nm, was determined for apoA-I-(44−186) in the presence of the indicated amounts of guanidine hydrochloride.

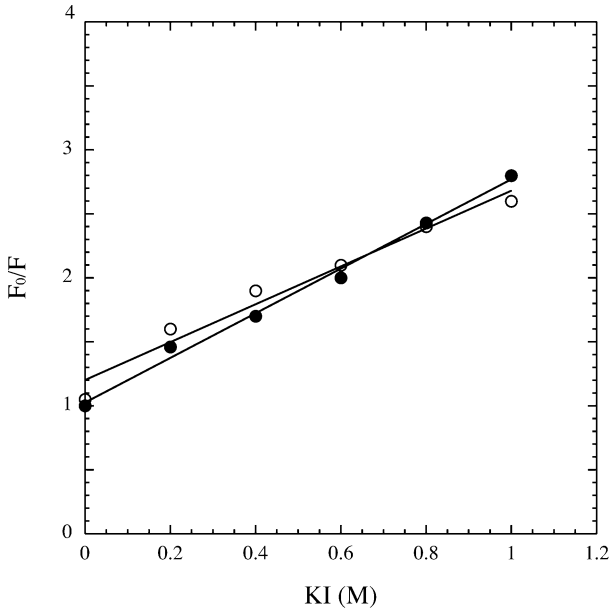

FIGURE 4: Stern−Volmer plots of tryptophan fluorescence quenching of wild-type apoA-I (open circles) and apoA-I-(44−186) (filled circles) by KI. The solvent employed was 20 mM sodium phosphate, pH 7.0.

truncated apoA-I is missing the first of these Trp residues. The similar quenching behavior observed, together with a 3 nm red shift in wavelength of maximum fluorescence emission, indicates that the relative exposure of Trp residues did not change significantly as a result of the dual N- and C-terminal truncation. Furthermore, the observed K_{sv} value is consistent with sequestration of Trp residues in apoA-I-(44−186) from the aqueous milieu.

Stryer (*17*) reported that the fluorescent dye ANS represents a useful reagent to evaluate the exposure of hydrophobic sites on proteins. To determine the extent to which truncation of apoA-I altered the exposure of hydrophobic regions of the protein, the effect of apoA-I-(44−186) and full-length apoA-I on ANS fluorescence emission intensity

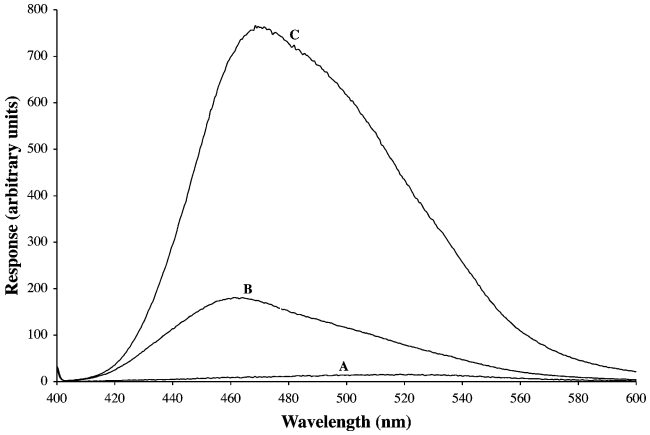

FIGURE 5: Effect of apolipoproteins on ANS fluorescence emission intensity. ANS (250 μM) in 20 mM sodium phosphate, pH 7.0, and 150 mM NaCl was excited at 395 nm, and emission was monitored from 400 to 600 nm. Curves: (A) ANS alone; (B) ANS plus 3 μM wild-type apoA-I; (C) ANS plus 3 μM apoA-I-(44−186).

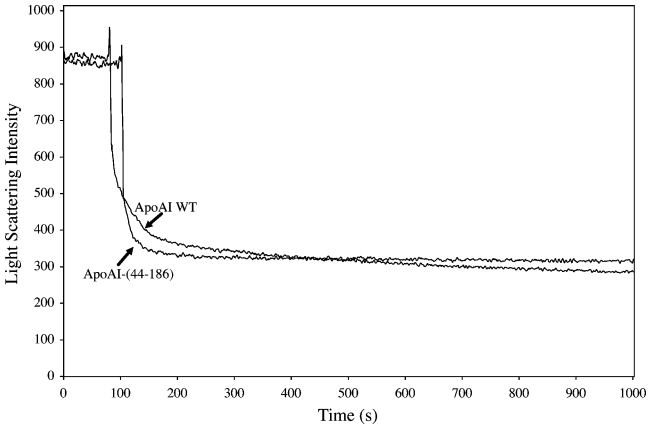

FIGURE 6: Effect of apolipoproteins on the light scattering intensity of DMPC vesicles. DMPC vesicles (600 nmol of phospholipid) were incubated in buffer at 24 °C at pH 7.0. Sample right angle light scatter intensity was monitored as a function of time. Curves: DMPC vesicles plus 6 nmol of apoA-I-(44−186); DMPC plus 6 nmol of wild-type apoA-I. The sharp positive response at approximately 100 s corresponds to the time at which the apolipoprotein was added.

was examined (Figure 5). In the absence of protein, ANS has a low quantum yield with an emission wavelength maximum of 515 nm (excitation 395 nm). Introduction of full-length apoA-I induced a 35 nm blue shift in ANS fluorescence emission wavelength maximum together with an enhancement in quantum yield. ApoA-I-(44−186) induced a similar blue shift in ANS fluorescence emission wavelength maximum as well as a greater enhancement in quantum yield. Given that these incubations contained equivalent molar amounts of apolipoprotein in an excess of ANS, the data indicate that apoA-I-(44−186) possesses more ANS-accessible hydrophobic binding sites than intact apoA-I.

Lipid Binding Studies. The kinetics of apoA-I-(44−186)-mediated DMPC vesicle solubilization was monitored as a function of time by right angle light scattering intensity measurements (Figure 6). ApoA-I-(44−186) and full-length apoA-I induced a time-dependent decrease in light scattering intensity with similar initial rates. Thus, despite loss of the C-terminal segment previously identified as the main lipid interaction site in apoA-I (*3*), the present combined N- and

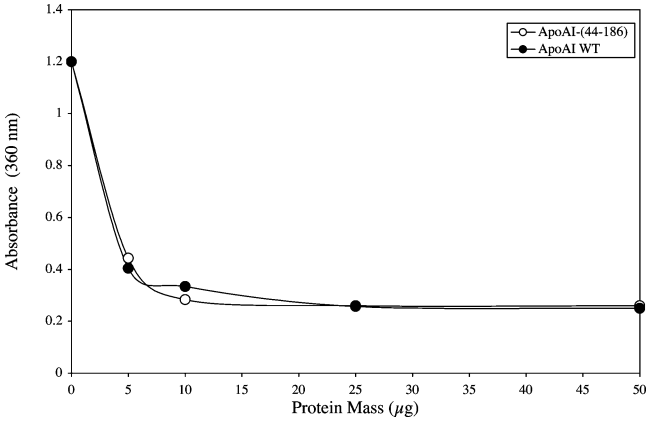

FIGURE 7: Effect of apolipoproteins on PL-C-induced aggregation of human LDL. Human LDL (50 μg of protein) and PL-C (0.33 unit) were incubated in the presence of specified amounts of wild-type apoA-I (filled circles) or apoA-I-(44−186) (filled squares). Sample absorbance at 340 nm was determined after 60 min.

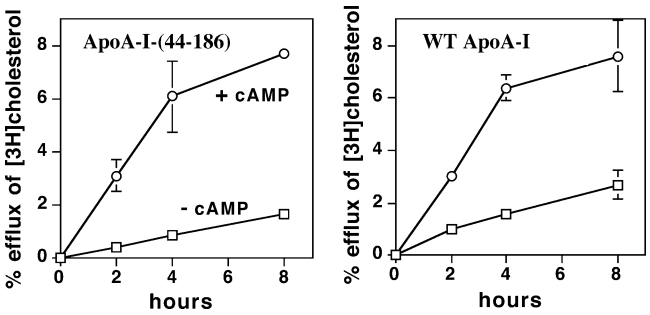

FIGURE 8: Effect of apoA-I-(44−186) on ABCA1-mediated cellular cholesterol efflux. J774 macrophages were incubated for 12 h with (circles) and without (squares) a cAMP analogue to upregulate ABCA1 protein expression. The ability of truncated apoA-I-(44−186) to stimulate cholesterol efflux is shown in the left panel and cholesterol efflux mediated by wild-type apoA-I in the right panel. Both acceptors were used in lipid-free form at a concentration of 50 μg/mL. Values are the mean ± SD, $n = 3$. Error bars are smaller than symbols when not seen.

C-terminal truncation variant manifests DMPC vesicle solubilization activity similar to intact apoA-I. When prepared on a preparative scale, apoA-I-(44−186)−DMPC complexes displayed flotation and native PAGE behavior characteristic of reconstituted HDL disks.

The lipoprotein binding properties of apoA-I-(44−186) were evaluated by determining its ability to prevent aggregation of human LDL induced by PL-C. Incubation of LDL with PL-C in the absence of apolipoprotein induces a time-dependent increase in sample turbidity, reaching a maximum by 1 h. Inclusion of increasing concentrations of apoA-I-(44−186) or wild-type apoA-I resulted in a concentration-dependent protection from PL-C-induced sample turbidity development (Figure 7) through formation of a stable binding interaction with the lipolyzed lipoprotein substrate (*24*).

Cholesterol Efflux Properties of ApoA-I-(44−186). ApoA-I is known to stimulate efflux of cholesterol from cells through interaction with the ABCA1 transporter. As shown in Figure 8, both apoA-I-(44−186) and full-length apoA-I support ABCA1-dependent cholesterol efflux from cultured macrophages. Furthermore, upregulation of ABCA1 by cAMP induced an increase in cholesterol efflux for both proteins, demonstrating that apoA-I-(44−186) is capable of serving as an acceptor of cell-derived cholesterol via ABCA1.

DISCUSSION

ApoA-I is a structurally resilient molecule that adapts to environmental conditions to fulfill its biological roles as acceptor of ABCA1-mediated cholesterol efflux, structural component of HDL, activator of LCAT, and ligand for the class B scavenger receptor. By analogy to other well-characterized apolipoproteins and on the basis of experimental evidence, it has been proposed that the N-terminus of human apoA-I adopts an amphipathic α-helix bundle conformation in the lipid-free state (*2*, *26*). The presence of such a structural entity in lipid-free apoA-I would permit sequestration of hydrophobic lipid binding surfaces from the aqueous milieu through helix−helix interactions. By the same token, lipid association-induced opening of the helix bundle would present helix segments to the surface without disruption of helix boundaries or large changes in helix content. Complicating this model, however, is the presence of a distinct C-terminal segment with high lipid binding affinity that is responsible for apoA-I oligomerization in the absence of lipid. In addition, N-terminal residues 1−43 appear to interact with the C-terminal segment and may adopt a unique tertiary fold (*11*). In considering the wealth of data obtained from various N- or C-terminal truncation mutants, we hypothesized that the central region of apoA-I may exist as a helix bundle in isolation. To test this hypothesis, we reengineered a plasmid vector optimized for bacterial expression of human apoA-I (*15*). The resulting construct, which encodes residues 44−186, was used to produce the truncated variant in *Escherichia coli*.

To evaluate the self-association properties of truncated apoA-I, sedimentation equilibrium experiments were conducted by analytical ultracentrifugation. The results revealed that apoA-I-(44−186) does not form higher order oligomers but rather exists in solution predominantly as a dimer. Although the sedimentation equilibrium data were fitted to a monomer−dimer−tetramer model, the apparent weight average molecular weight was that of the dimer, and there was no concentration dependency at the three loading concentrations and three speeds employed, suggesting predominance of a single species. This was reinforced by sedimentation velocity experiments carried out at the highest sedimentation equilibrium loading concentration. These data, best fit by a single species model, were used to evaluate the overall shape of the apoA-I-(44−186) dimer. From the sedimentation coefficient and hydration values, using a prolate model and a hydration expansion of 17.1%, an axial ratio (a/b) = 4.2 was calculated. Whereas this value is less than that observed for full-length apoA-I (*27*), this may be explained by the combined effects of truncation and dimerization, both of which would be expected to decrease the overall asymmetry observed. Although the nature of the dimer interface in apoA-I-(44−186) remains to be established, the data suggest that the combined N- and C-terminal truncation introduced here does not preclude the remaining portion of the protein to attain an asymmetric globular protein fold. By contrast, N-terminal deletion alone induces a large structural reorganization to a conformation that resembles the lipid-bound state of the protein (*5*). This is consistent with the concept that N-terminus−C-terminus interactions function in maintenance of the global fold of apoA-I in the lipid-free state (*11*, *26*, *28*). Deletion of the extreme

C-terminus eliminates the region of the protein that serves as the primary trigger of apoA-I lipid binding-induced conformational changes (*12*). At the same time, removal of the N-terminus induces a conformational change because the deleted segment is not available to interact with the C-terminus and, thereby, stabilize its lipid-free conformation. It is plausible to consider that lack of an intramolecular binding partner for the C-terminus (i.e., the N-terminus) induces a global conformational transition that resembles the lipid-associated conformation of this protein. The present results, however, suggest that combined removal of both segments permits the residual core structure to retain its "lipid-free" conformation.

Far-UV circular dichroism spectroscopy was performed to characterize the secondary structure content of apoA-I-(44−186). In buffer at pH 7.0 the truncated protein manifests 65% α-helix, consistent with secondary structure prediction analysis of full-length apoA-I (*4*). These data are also consistent with the concept that combined N- and C-terminal truncation yields a core protein fragment whose structural organization reflects the conformation it adopts in the context of the intact protein. To evaluate the effect of combined N- and C-terminal truncation on the stability of apoA-I-(44−186), guanidine hydrochloride denaturation studies were performed. Compared to full-length apoA-I, apoA-I-(44−186) was less resistant to denaturation, displaying a transition midpoint of 0.5 M guanidine hydrochloride versus 1.0 M for full-length apoA-I (*29*). The decreased resistance to unfolding of apoA-I-(44−186) suggests that one or both of the deleted segments exert a stabilizing effect on the central region of the protein.

A feature of known helix bundle apolipoproteins is a characteristic response to the lipid mimetic cosolvent, trifluoroethanol. Trifluoroethanol has previously been shown to induce α-helix structure in lipid-free apoA-I, as seen by a significant increase in negative ellipticity, especially at 208 nm (*30*). Others (*31*−*34*) have shown that the ratio of ellipticity at 222 nm to 208 nm can be used to evaluate the existence of interhelical contacts in coiled coil peptides. Since exchangeable apolipoproteins contain predominantly α-helical secondary structure, they are suitable candidates for this analysis. In known helix bundle apolipoproteins, the 222 nm/208 nm ellipticity ratio value approaches 1.0 in buffer. In 50% trifluoroethanol (v/v), however, a decrease in the corresponding ratio is observed (*35*), consistent with trifluoroethanol-induced disruption of hydrophobic contacts between neighboring amphipathic α-helices. In buffer at pH 7.0 apoA-I-(44−186) manifests a 208/222 nm ellipticity ratio of 0.97 while this value decreases to 0.87 in the presence of trifluoroethanol. The observation that N- and C-terminal truncated apoA-I follows the same pattern displayed by apolipoproteins known to exist as globular amphipathic α-helix bundles (*36*−*38*) provides support for the concept that helix−helix contacts, possibly as an amphipathic α-helix bundle, exist in apoA-I-(44−186). Given the fact that apoA-I(44−186) exists in solution predominantly as a dimer, however, intermolecular helix−helix interactions may also contribute to the observed changes in ellipticity ratio. Fluorescence quenching studies revealed that, despite loss of one of the four Trp residues present in full-length apoA-I and deletion of 100 amino acids, the relative exposure of Trp residues to the negatively charged quenching agent, KI, were similar. Thus, the conformation adopted by the remaining core fragment of apoA-I was not reflective of a major structural alteration in the protein. Despite this, fluorescent dye binding experiments revealed an increase in exposed hydrophobic surface upon truncation of apoA-I. Notwithstanding differences in protein sequence, combined N- and C-terminal truncation results in a conformation that manifests decreased sequestration of hydrophobic sites on the protein compared to its full-length counterpart.

To evaluate the ability of apoA-I-(44−186) to interact with lipid surfaces, phospholipid vesicle solubilization experiments were performed. Both truncated and full-length apoA-I induced a time-dependent decrease in DMPC vesicle light scattering intensity, coincident with conversion of the vesicles into protein−lipid complexes. The comparable vesicle solubilization activities observed are noteworthy in light of the fact that the C-terminus of apoA-I is recognized as the major lipid binding element in the protein (*3*). One possible explanation for this may be related to the observed decrease in apoA-I-(44−186) stability in buffer compared to full-length apoA-I. In other systems it has been shown that adoption of molten globule-like properties enhances the lipid interaction ability of apolipoproteins (*25*, *39*). If deletion of N- and/or C-terminal stabilizing elements results in a central helix bundle that is less stable in solution, it would be expected to display enhanced lipid surface activity. These studies were extended by examining the lipoprotein binding activity of apoA-I-(44−186). The observation that truncated apoA-I and full-length apoA-I display similar abilities to protect isolated human LDL from aggregation induced by exposure to PL-C provides further evidence that the present combined N- and C-terminal truncation did not destroy the lipid binding ability of apoA-I. These results, however, differ from data reported by Fang et al. (*40*). These authors found that apoA-I-(42−184) was unable to interact with DMPC vesicles to generate disk complexes (*40*). The reason for the discrepancy with results reported herein is unclear but may be related to the specific incubation conditions employed. Another possibility is that subtle differences in the nature of the truncation (residues 42−184 in one case versus residues 44−186 in the other) may be responsible although, given the very close similarity between these sequences, this interpretation seems unlikely. Finally, the differences observed between these studies may be related to the differences observed in the secondary structure content of the two preparations. Whereas truncated apoA-I employed in the present study possessed 65% α-helix secondary structure, the preparation employed by Fang et al. (*26*) displayed considerably less α-helix (37%). Thus, it is conceivable that differences in secondary structure content between the two preparations are related to the disparate lipid binding capabilities of these proteins. If the preparation of Fang et al. was misfolded or partially misfolded, then this could be responsible for the lower ellipticity values they observed as well as the apparent lack of lipid binding activity. The results of the present study, wherein apoA-I-(44−186) efficiently solubilized phospholipid vesicles, bound to modified lipoproteins, and supported ABCA1-dependent cholesterol efflux, strongly suggest that this truncated protein is functional in terms of lipid binding activity. With regard to the cholesterol efflux experiments, the observed capability of apoA-I-(44−186) to support ABCA1-dependent cholesterol efflux was

surprising in light of the observation (*41*) that the terminal helix in wild-type apoA-I (helix 10) plays an important role in its efflux capacity. It is possible that a different structural element, which is conserved in apoA-I-(44−186), is capable of substituting for the proposed function of helix 10 in full-length apoA-I.

In conclusion, accumulating evidence (*1*, *2*) suggests that the central region in lipid-free apoA-I can exist as an independently folded functional fragment of apoA-I. In the present study results obtained from very different analyses, including hydrodynamic experiments, far-UV CD spectroscopy, fluorescence spectroscopy, and lipid binding activity, are consistent with this interpretation. In future studies, it will be important to establish the precise tertiary organization of this region of apoA-I. Knowledge of individual amphipathic α-helix boundaries, for example, will provide needed insight into the mechanism of lipid binding and generation of nascent HDL particles, an integral process in the reverse cholesterol transport pathway.

ACKNOWLEDGMENT

The authors thank Emmanuel Guigard for hydrodynamic studies and Robert Luty for circular dichroism analysis.

REFERENCES

1. Davidson, W. S., Arnvig-McGuire, K., Kennedy, A., Kosman, J., Hazlett, T. L., and Jonas, A. (1999) Structural organization of the N-terminal domain of apolipoprotein A-I: studies of tryptophan mutants, *Biochemistry 38*, 14387−14395.
2. Saito, H., Dhanasekaran, P., Nguyen, D., Holvoet, P., Lund-Katz, S., and Phillips, M. C. (2003) Domain structure and lipid interaction in human apolipoproteins A-I and E, a general model, *J. Biol. Chem. 278*, 23227−23232.
3. Ji, Y., and Jonas, A. (1995) Properties of an N-terminal proteolytic fragment of apolipoprotein AI in solution and in reconstituted high-density lipoproteins, *J. Biol. Chem. 270*, 11290−11297.
4. Segrest, J. P., Jones, M. K., De Loof, H., Brouillette, C. G., Venkatachalapathi, Y. V., and Anantharamaiah, G. M. (1992) The amphipathic helix in the exchangeable apolipoproteins: a review of secondary structure and function, *J. Lipid Res. 33*, 141−166.
5. Rogers, D. P., Brouillette, C. G., Engler, J. A., Tendian, S. W., Roberts, L., Mishra, V. K., Anantharamaiah, G. M., Lund-Katz, S., Phillips, M. C., and Ray, M. J. (1997) Truncation of the amino terminus of human apolipoprotein A-I substantially alters only the lipid-free conformation, *Biochemistry 36*, 288−300.
6. Rogers, D. P., Roberts, L. M., Lebowitz, J., Engler, J. A., and Brouillette, C. G. (1998) Structural analysis of apolipoprotein A-I: effects of amino- and carboxy-terminal deletions on the lipid-free structure, *Biochemistry 37*, 945−955.
7. Borhani, D. W., Rogers, D. P., Engler, J. A., and Brouillette, C. G. (1997) Crystal structure of truncated human apolipoprotein A-I suggests a lipid-bound conformation, *Proc. Natl. Acad. Sci. U.S.A. 94*, 12291−12296.
8. Koppaka, V., Silvestro, L., Engler, J. A., Brouillette, C. G., and Axelsen, P. H. (1999) The structure of human lipoprotein A-I. Evidence for the "belt" model, *J. Biol. Chem. 274*, 14541−14544.
9. Li, H., Lyles, D. S., Thomas, M. J., Pan, W., and Sorci-Thomas, M. G. (2000) Structural determination of lipid-bound ApoA-I using fluorescence resonance energy transfer, *J. Biol. Chem. 275*, 37048−37054.
10. Davidson, W. S., and Hilliard, G. M. (2003) The spatial organization of apolipoprotein A-I on the edge of discoidal high-density lipoprotein particles: a mass spectrometry study, *J. Biol. Chem. 278*, 27199−27207.
11. Tricerri, M. A., Behling, A. K., Sanchez, S. A., and Jonas, A. (2000) Characterization of apolipoprotein A-I structure using a cysteine-specific fluorescence probe, *Biochemistry 39*, 14682−14691.
12. Oda, M. N., Forte, T. M., Ryan, R. O., and Voss, J. C. (2003) The C-terminal domain of apolipoprotein A-I contains a lipid-sensitive conformational trigger, *Nat. Struct. Biol. 10*, 455−460.
13. Weisgraber, K. H. (1994) Apolipoprotein E: structure−function relationships, *Adv. Protein Chem. 45*, 249−302.
14. Narayanaswami, V., and Ryan, R. O. (2000) Molecular basis of exchangeable apolipoprotein function, *Biochim. Biophys Acta 1483*, 15−36.
15. Ryan, R. O., Forte T. M., and Oda, M. N. (2003) Optimized bacterial expression of human apolipoprotein A-I, *Protein Exprression Purif. 27*, 98−103.
16. Oda, M. N., Bielicki, J. K., Berger, T., and Forte, T. M. (2001) Cysteine substitutions in apolipoprotein A-I primary structure modulate paraoxonase activity, *Biochemistry 40*, 1710−1718.
17. Stryer, L. (1965) The interaction of a naphthalene dye with apomyoglobin and apohemoglobin. A fluorescent probe of non-polar binding sites, *J. Mol. Biol. 13*, 482−495.
18. Laue, T. M., and Stafford, W. F., III (1999) Modern applications of analytical ultracentrifugation, *Annu. Rev. Biophys. Biomol. Struct. 28*, 75−100.
19. Johnson, M. L., Correia, J. J., Yphantis, D. A., and Halvorson, H. R. (1981) Analysis of data from the analytical ultracentrifuge by nonlinear least-squares techniques, *Biophys. J. 36*, 575−588.
20. Laue, T. M., Shah, B. D., Ridgeway, T. M., and Pelletier, S. L. (1991) in *Analytical Ultracentrifugation in Biochemistry and Polymer Science* (Harding, S. E., Rowe, A. J., and Horton, J. C., Eds.) pp 90−125, Royal Society of Chemistry, Cambridge, U.K.
21. Babul, J., and Stellwagen, E. (1969) Measurement of protein concentration with interferences optics, *Anal. Biochem. 28*, 216−221.
22. Provencher, S. W., and Glöckner, J. (1981) Estimation of globular protein secondary structure from circular dichroism, *Biochemistry 20*, 33−37.
23. Weers, P. M. M., Narayanaswami, V., Kay, C. M., and Ryan, R. O. (1999) Interaction of an exchangeable apolipoprotein with phospholipid vesicles and lipoprotein particles. Role of leucines 32, 34, and 95 in *Locusta migratoria* apolipophorin III, *J. Biol. Chem. 274*, 21804−21810.
24. Liu, H., Scraba, D. G, and Ryan, R. O. (1993) Prevention of phospholipase-C induced aggregation of low-density lipoprotein by amphipathic apolipoproteins, *FEBS Lett. 316*, 27−33.
25. Soulages, J. L., and Bendavid, O. J. (1998) The lipid binding activity of the exchangeable apolipoprotein apolipophorin-III correlates with the formation of a partially folded conformation, *Biochemistry 37*, 10203−10210.
26. Fang, Y., Gursky, O., and Atkinson, D. (2003) Structural studies of N- and C-terminally truncated human apolipoprotein A-I, *Biochemistry 42*, 6881−6890.
27. Edelstein, C., and Scanu, A. M. (1980) Effect of guanidine hydrochloride on the hydrodynamic and thermodynamic properties of human apolipoprotein A-I in solution, *J. Biol. Chem. 255*, 5747−5754.
28. Behling-Agree, A. K., Tricerri, M. A., Arnvig-McGuire, K., Tian, S. M., and Jonas, A. (2002) Folding and stability of the C-terminal half of apolipoprotein A-I examined with a Cys-specific fluorescence probe, *Biochim. Biophys. Acta 1594*, 286−296.
29. Reijngoud, D. J., and Phillips, M. C. (1982) Mechanism of dissociation of human apolipoprotein A-I from complexes with dimyristoylphosphatidylcholine as studied by guanidine hydrochloride denaturation, *Biochemistry 21*, 2969−2976.
30. Ryan, R. O., Yokoyama, S., Liu, H., Czarnecka, H., Oikawa, K., and Kay, C. M. (1992) Human apolipoprotein A-I liberated from high-density lipoprotein without denaturation, *Biochemistry 31*, 4509−4514.
31. Chao, H., Houston, M. E., Jr., Grothe, S., Kay, C. M., O'Connor-McCourt, M., Irvin, R. T., and Hodges, R. S. (1996) Kinetic study on the formation of a de novo designed heterodimeric coiled-coil: use of surface plasmon resonance to monitor the association and dissociation of polypeptide chains, *Biochemistry 35*, 12175−12185.
32. Cooper, T. M., and Woody, R. W. (1990) The effect of conformation on the CD of interacting helices: a theoretical study of tropomyosin, *Biopolymers 30*, 657−676.
33. Hodges, R. S., Semchuk, P. D., Taneja, A. K., Kay, C. M., Parker, J. M. R., and Mant, C. T. (1988) Protein design using model synthetic peptides, *Pept. Res. 1*, 19−30.
34. Lau, S. Y. M., Taneja, A. K., and Hodges, R. S. (1984) Synthesis of a model protein of defined secondary and quaternary structure.

Effect of chain length on the stabilization and formation of two-stranded alpha-helical coiled-coils, *J. Biol. Chem. 259*, 13253−13261.
35. Kiss, R. S., Kay, C. M., and Ryan, R. O. (1999) Amphipathic α-helix bundle organization of lipid-free chicken apolipoprotein A-I, *Biochemistry 38*, 4327−4334.
36. Wilson, C., Wardell, M. R., Weisgraber, K. H., Mahley, R. W., and Agard, D. A. (1991) Three-dimensional structure of the LDL receptor-binding domain of human apolipoprotein E, *Science 252*, 1817−1822.
37. Breiter, D. R., Kanost, M. R., Benning, M. M., Wesenberg, G., Law, J. H., Wells, M. A., Rayment, I., and Holden, H. M. (1991) Molecular structure of an apolipoprotein determined at 2.5-Å resolution, *Biochemistry 30*, 603−608.
38. Wang, J., Sykes, B. D., and Ryan, R. O. (2002) Structural basis for the conformational adaptability of apolipophorin III, a helix-bundle exchangeable apolipoprotein, *Proc. Natl. Acad. Sci. U.S.A. 99*, 1188−1193.
39. Morrow, J. A., Hatters, D. M., Lu, B., Hochtl, P., Oberg, K. A., Rupp, B., and Weisgraber, K. H. (2002) Apolipoprotein E4 forms a molten globule. A potential basis for its association with disease, *J. Biol. Chem. 277*, 50380−50385.
40. Fang, Y., Gursky, O., and Atkinson, D. (2003) Lipid-binding studies of human apolipoprotein A-I and its terminally truncated mutants, *Biochemistry 42*, 13260−13268.
41. Panagotopulos, S. E., Witting, S. R., Horace, E. M., Hui, D. Y., Maiorano, J. N., and Davidson, W. S. (2002) The role of apolipoprotein A-I helix 10 in apolipoprotein-mediated cholesterol efflux via the ATP-binding cassette transporter ABCA1, *J. Biol. Chem. 277*, 39477−39484.

BI0477135